Received: 18 May 2016 | Accepted: 15 August 2016

DOI: 10.1111/cpr.12293

ORIGINAL ARTICLE

WILEY Cell Proliferation

Loss of TAB3 expression by shRNA exhibits suppressive bioactivity and increased chemical sensitivity of ovarian cancer cell lines *via* the NF-κB pathway

Yannan Chen[1†] | Xia Wang[2†] | Chengwei Duan[3] | Jie Chen[4] | Ming Su[1] | Yunfeng Jin[1] | Yan Deng[1] | Di Wang[1] | Caiwen Chen[5] | Linsen Zhou[6] | Jialin Cheng[1] | Wei Wang[1] | Qinghua Xi[1]

[1]Department of Obstetrics and Gynecology, Affiliated Hospital of Nantong University, Nantong University, Nantong, Jiangsu, China

[2]Center For Reproductive Medicine, Affiliated Hospital of Nantong University, Nantong University, Nantong, Jiangsu, China

[3]Department of Science and Education, the Second People's Hospital of Nantong, Jiangsu, China

[4]Department of Oncology, Jiangyin People's Hospital, Jiangyin, Jiangsu, China

[5]Department of Obstetrics and Gynecology, Yixing People's Hospital, Wuxi, Jiangsu, China

[6]Department of Obstetrics and Gynecology, Affiliated Maternal and Child Care Service Centre, Nantong, Jiangsu, China

Correspondence
Qinghua Xi, Department of Obstetrics and Gynecology, Affiliated Hospital of Nantong University, Nantong University, Nantong, Jiangsu, China.
Email: ntdxfsyyxqh@126.com

Abstract

Ovarian cancer is a leading cause of death among gynaecologic malignancies. Despite many years of research, it still remains sparing in reliable diagnostic markers and methods for early detection and screening. Transforming growth factor β-activated protein kinase 1 (TAK1)-binding protein 3 (TAB3) was initially characterized as an adapter protein essential for TAK1 activation in response to IL-1β or TNFα, however, the physiological role of TAB3 in ovarian cancer tumorigenesis is still not fully understood. In this study, we evaluated the effects of TAB3 on ovarian cancer cell lines. Expressions of TAB3 and PCNA (proliferating cell nuclear antigen) were found to be gradually increased in EOC tissues and cell lines, by western blot analysis and qRT-PCR. Distribution of TAB3 was further analysed by immunohistochemistry. *In vitro*, knockdown of TAB3 expression in HO8910 or SKOV3 ovarian cancer cells significantly inhibited bioactivity of ovarian cancer cells, including proliferation and cell-cycle distribution, and promoted chemical sensitivity to cisplatin and paclitaxel treatment *via* inhibiting NF-κB pathways. In conclusion, our study strongly suggests a novel function of TAB3 as an oncogene that could be used as a biomarker for ovarian cancer. It provides a new insight into the potential mechanism for therapeutic targeting, in chemotherapy resistance, common in ovarian cancer.

1 | INTRODUCTION

In stark contrast to other cancers, the survival rate for ovarian cancer has not changed significantly in the last 30 years.[1] It is still the second cause of death among female reproductive malignancies with an estimated 21 290 new cases diagnosed and 14 180 deaths in the United States in 2015.[2] In the early stage, ovarian cancers show vague symptoms or are asymptomatic. Thus, most ovarian cancers are detected at advanced stages, while cancer has spread beyond the primary tumour site.[3] Nowadays, the standard treatment for ovarian cancer is the surgical "debulking" followed by chemotherapy, usually a combination of platinum-based drugs such as cisplatin or oxaliplatin, alongside a taxane such as paclitaxel.[4] Therefore, to extend the lifespan of patients with ovarian cancer, further research into the molecular changes underpinning the disease needs to be conducted. What is more, once pathways are identified, specific biomarkers need to be pursued and robustly investigated to determine their potential as drug targets.[5]

Among canonical signal pathways involved in tumour progression, nuclear factor κB (NF-κB) is a family of transcription factors that plays pivotal roles in various cellular processes, including immunity,

[†]Yannan Chen and Xia Wang contributed equally to this work.

inflammation, carcinogenesis and chemoresistance.[6] NF-κB family consists of five structurally related proteins, p65, p105/p50, p100/p52, RelB and c-Rel. The predominant ones among them consists of p50 and p65 subunits.[7] In the resting state, NF-κB is normally sequestered in the cytoplasm by association with inhibitory IκB proteins. Once stimulated, it is phosphorylated, ubiquitinated and subsequent proteasome-mediated degradation. This results in the release of NF-κB and nuclear translocation of p65–p50 complex, where it activates transcription of target genes.[8,9] To date, it is reported that besides chronic inflammatory and autoimmune disease, cancer development is also closely associated with excessive activation of NF-κB signalling pathway. The chemotherapy-induced DNA damage can activate NF-κB in some cell contexts.[10]Many potent anti-apoptosis genes are transactivated by NF-κB.[11] Hence, the precise regulation of NF-κB signalling pathway is indispensable and may aid the identification of novel therapeutic targets for cancer.

Ubiquitination or phosphorylation-mediated signalling transductions are important regulatory mechanisms for the activation of NF-κB.[12] As the major adaptor protein family in the NF-κB activation, TAB3 links TRAFs molecular *via* ubiquitin chain to activate TAK1.[13,14] TAB3 contains a highly conserved C-terminal novel zinc finger domain, which binds preferentially to Lys63-linked polyubiquitin chains. Importantly, TAB3 is markedly elevated in a variety of cancers and silenced TAB3 could enhance the rates of doxorubicin-induced apoptosis and the chemosensitivity of hepatocellular carcinoma cells.[15] In addition, knockdown of TAB3 inhibits NF-κB-induced NSCLC proliferation and chemoresistance, indicating that TAB3 might represent as a potential anti-cancer target.[16] What is more, in triple negative breast cancer, TAB3 can promote its metastasis by triggering TAK1 mediated NF-κB activation.[17] However, whether TAB3 is involved in the progress of ovarian cancer is enigmatic.

In this study, we sought to analyse TAB3 expression levels in ovarian cancer tissues and cells and evaluate the correlations between TAB3 expression and clinicopathological features, as well as its implication for clinical prognosis. Using the cell lines HO8910 and OVCAR3, as well as clinical samples and publically available algorithms, we found that TAB3 regulated the NF-κB pathway and thereby promoted cell proliferation and chemoresistance in ovarian cancer. Better understanding of the molecular mechanism of TAB3 may, therefore, provide new insights into the pathophysiology of ovarian cancer and uncover its potential for diagnosis and management of the disease.

2 | MATERIALS AND METHODS

2.1 | Patients and tissue samples

EOC tissues were obtained from 119 patients who underwent surgical resection without preoperative chemotherapy in the surgery department. Informed consent for tissue use was obtained from all patients. Tumour samples were graded based on Gynaecologic Oncology Group Criteria and staged in accordance with the FIGO system. Patient follow-up was terminated on 2 October 2015. Average follow-up time was 47.20 months (median 54.0; range 3–60). Patients alive at the end of follow-up were censored. For the histological examinations, all the tumorous and surrounding non-tumorous tissue portions were fixed in formalin and embedded in paraffin. To determine factors influencing survival after operation, couples of conventional variables along with the expression of TAB3 were tested in all participants. The Ethics Committee of Affiliated Hospital of Nantong University had authorized us to use the tissue sections for research. The main clinical and pathologic variables of the patients are shown in Table 1.

2.2 | Cell lines and cell culture

The A2780, HO8910, OVCAR3, SKOV3 and IOSE80 cell lines were purchased from Xiangya Medical College (Changsha, China). The cells were maintained in DMEM (Invitrogen, Carlsbad, CA, USA) supplemented with 10% foetal bovine serum (FBS) at 37°C in a humidified atmosphere containing 5% CO_2.

2.3 | Reagents and antibodies

Anti-TAB3(sc-166538), anti-Ki67(sc-23900), anti-PCNA(sc-25280), anti-GAPDH (sc-166574), anti-IκBα (sc-371), anti-p65(sc-126)

TABLE 1 The connection between TAB3 and clinicopathological parameters in 119 EOC specimens

		TAB3 expression			
Parameters	**Total**	**Low**	**High**	***P* value[a]**	**χ^2 value**
Age (24–80 years, mean 55 years)					
≤50	40	19	21	.951	0.004
>50	79	38	41		
Histologic subtype					
Serous	64	30	34	.704	1.406
Mucinous	26	14	12		
Endometrioid	15	8	7		
Clear cell	14	5	9		
Histological grade					
Low	53	31	22	.038*	4.295
High	66	26	40		
FIGO stage					
I/II	59	42	17	.000*	25.428
III/IV	60	15	45		
Lymph node metastasis					
Negative	74	43	31	.004*	8.173
Positive	45	14	31		
Ki-67 expression					
Low	52	31	21	.024*	5.080
High	67	26	41		

[a]Statistical analyses were performed by the Pearson χ^2 test.
*P<.05 was considered significant.

and anti-phosphop65 (Ser536) (sc-101752) were from Santa Cruz Biotechnology (Santa Cruz, CA, USA). Anti-phosphoIKKα/β (Serl76/180) (sc-2679) and anti-phospho-IκBα(Ser32) were from Cell Signaling Technology (Boston, Massachusetts, USA). Enhanced chemiluminescence, western blotting detection reagents were purchased from Amersham (Arlington Heights, IL, USA). All other chemicals were purchased from Sigma (St. Louis, MO, USA).

2.4 | Western blotting

Cells were lysed in lysis buffer (20 mM Tris-HCL, 1 mM EGTA, 1 mM EDTA, 10 mM NaCl, 0.1 mM phenylmethylsulfonyl fluoride, 1 mM Na_3VO_4, 30 mM sodium pyrophosphate, 25 mM β-glycerol phosphate, 1% Triton X-100, pH 7.4). Cell lysates were centrifuged at 1500 rpm for 15 minutes at 4°C, and supernatants were used for Western blotting. Lysates were resolved by sodium dodecyl sulphate-polyacrylamide gel electrophoresis (SDS PAGE), transferred onto a nitrocellulose membrane and then stained with 0.1% Ponceau S solution (Sigma-Aldrich). After blocking with 5% non-fat milk, the membranes were immunoblotted with various antibodies overnight, and the bound antibodies were visualized with horseradish peroxidase-conjugated secondary antibodies, using the enhanced chemiluminescence Western blotting system (ECL; Amersham Biosciences (Fairfield, Connecticut, USA)).

2.5 | RNA extraction and RT-PCR

Total RNA was extracted from 80% to 90% confluent cultures using TRIzol reagent (Sigma) and reverse transcribed into cDNA using the Reverse Transcription cDNA Kit (#RT50KN; NanoHelix Co., Ltd (Seoul, South Korea)). cDNA in 1 μL of the reaction mixture was amplified using the Ready-2×-Go pre-mix PCR kit (#PMD008L; NanoHelix) and 10 pmol each of sense and antisense primers. The thermal cycle profile was as follows: denaturation at 95°C for 30 seconds, annealing at 54°C for 30 seconds depending on the primers used and extension at 72°C for 30 seconds. Each PCR reaction was carried out for 25–30 cycles. PCR products were analysed by 1% agarose gel electrophoresis.

2.6 | Immunohistochemistry staining

Five-micrometre-thick serial was mounted on glass slides coated with 10% polysine. Sections were dewaxed in xylene for 15 minutes twice and rehydrated in graded ethanols. Immunoreactivity was enhanced by a pressure cooker by incubating the tissue sections for 3 minutes in 0.1 M citrate buffer. The following panel of antibodies was used: TAB3 (Santa Cruz Biotechnology; 1:100 dilution) incubated for 4 hours at room temperature and Ki-67 (Santa Cruz Biotechnology; 1:500 dilution) incubated for 2 hours at room temperature. The sections were washed three times with phosphate-buffered saline (PBS). Then, diaminobenzidine was used for signal development, and the sections were counterstained with 20% haematoxylin. The slides were dehydrated, cleared and evaluated.

2.7 | Immunohistochemistry analysis

More than 500 cells were counted to determine the labelling index, which represented the percentage of immunostained cells relative to the total number of cells. The extent of staining was scored based on the percentage of positive tumour cells: 0 (negative and <5% of cells), 1 (5–25%), 2 (25–50%), 3 (50–75%) and 4 (>75%). The intensity of immunostaining in each tumour section was assessed as 0 (negative), 1 (weak), 2 (moderate), 3 (strong) and then a combination of these values. Scores ≤3 were considered low expression of TAB3 and those scores more than 3 were considered strongly positive for TAB3 overexpression.

2.8 | Transient transfection

The TAB3-shRNA and control-shRNA were purchased from Genechem (Shanghai, Japan). The TAB3-specific shRNA target sequences are as follows: TAB3-shRNA#1, 5′-CTGAGGAAATGACAAGATT-3′; TAB3-shRNA#2, 5′-GGTTGAAGTCTGAAGTTAA-3′; and TAB3-siRNA#3, 5′-CAACTTAATGGTGGTCGAA-3′. EOC cells were grown in dishes until they reached 80% confluence. The medium was replaced 6 hours later with fresh medium for transfection. HO8910 and SKOV3 cells were transfected with TAB3-shRNA or control-shRNA according to the manufacturer's instructions. Cells were collected for Western blot, MTT and flow cytometry assays after transfection for 36 hours.

2.9 | Cell proliferation assays

The EOC cells were plated and grown in 96-well plates at a concentration of 4000 cells/well for 24 hours. Cells were subsequently treated with varying plasmid for 36 hours. MTT (5 mg/mL) was added to the 96-well plates at 5 μL/well, followed by an additional hour of incubation. The MTT reaction was terminated through the addition of 100 μL of DMSO. The results were read by measuring absorption at 490 nm with a Microplate Reader (Tecan, Morrisville, NC, USA). Each experiment was performed in triplicate to assess for consistency of results.

2.10 | Cell-cycle analysis

Starvation and re-feeding were used to imitate cell cycle. First, we used 1640 medium without FBS to incubate HO8910 and SKOV3 cells for 48 hours to synchronize cells and then changed into complete medium. After that, we harvested cells at time point.

The effects of TAB3-shRNA and control-shRNA on cell-cycle progression were measured by Cellometer. Briefly, 2.5×10^5 cells/well were seeded into six-well plates, incubated overnight and then treated with varying plasmid for 36 hours. The cells were harvested and washed with phosphate-buffered saline (PBS). The pellet was re-suspended and fixed in 90% pre-chilled methanol and stocked overnight at −20°C. The cells were then washed with PBS again and resuspended in 50 μL RNase solution (250 μg/mL)

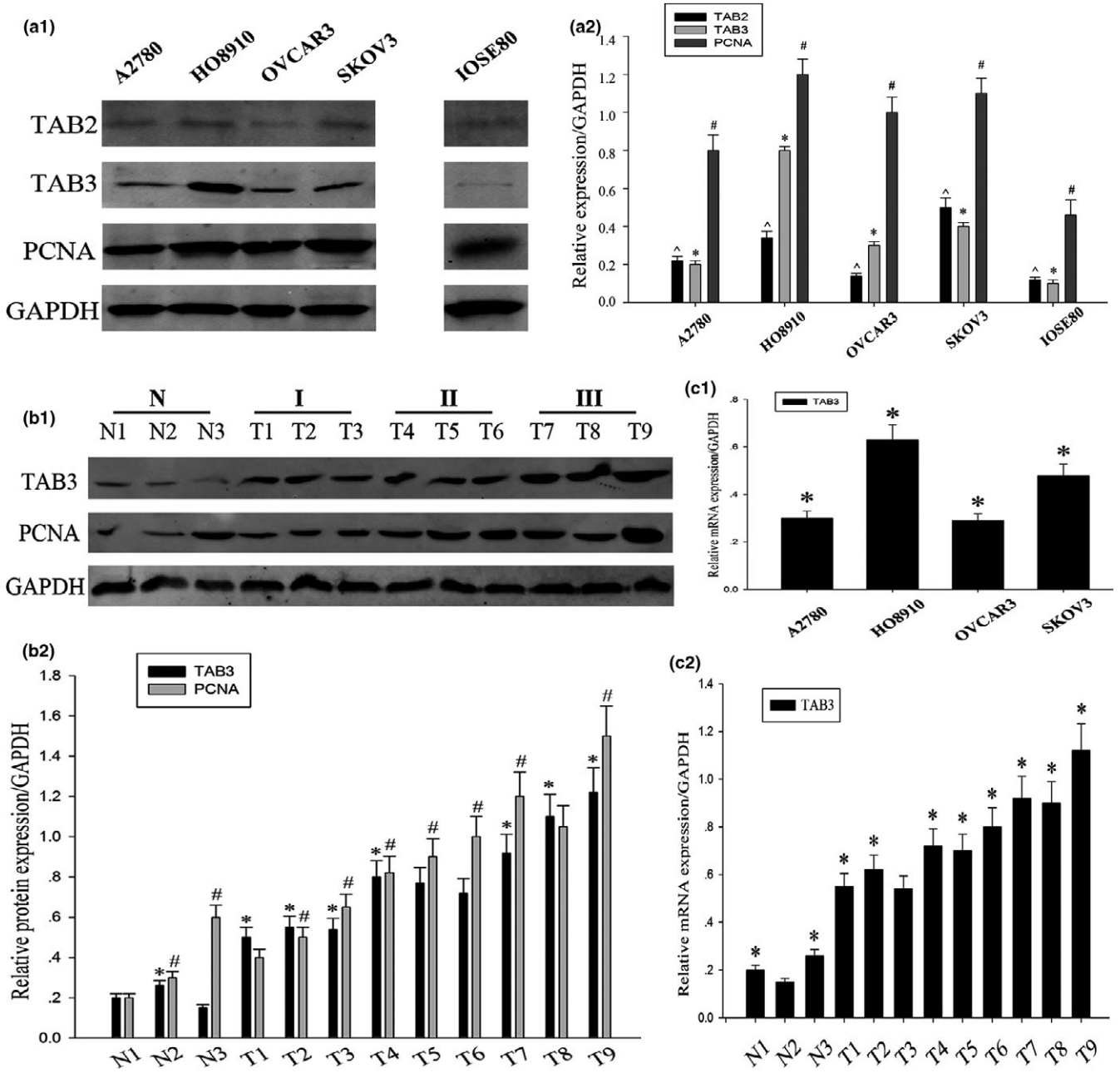

FIGURE 1 TAB3 expression was up-regulated in EOC tissues and cell lines. (a1 and a2) The expressions of TAB3 in four EOC cell lines (A2780, HO8910, OVCAR3 and SKOV3 as showed) and one normal ovarian cell line were examined by WB. **P*<.05. (B1 and B2) Western blotting (WB) was performed to detect TAB3 expression levels in three normal tissues (N1, N2 and N3) and nine EOC tissues (T1–T9) from grade 1 (I) to grade 3 (III) (N: normal; EOC: epithelial ovarian cancer; T: tumour). **P*<.05. (C1 and C2) The levels of TAB3 mRNA expression were evaluated in normal ovarian tissues and different EOC tissues and cell lines. **P*<.05. The relative expression levels were showed by density photometry and GAPDH was used as a loading control. The same experiment was repeated at least three times

and 10 mM EDTA for 30 minutes. Finally, 50 μL staining solution [containing 2 mg/mL PI (Biotium, Hayward, MA, USA), 0.1 mg/mL Azide (Sigma-Aldrich) and 0.05% Triton X-100 (Sigma-Aldrich)] was added, and the final mixture was incubated for 15 minutes in the dark before being analysed on Cellometer. The measured results were analysed using the FCS4 express software (Molecular Devices, Sunnyvale, CA, USA). Cell-cycle analysis assay was performed in duplicate.

2.11 | Immunofluorescence

The cells were fixed in 4% formaldehyde and incubated in 0.3% Triton X-100 (Sigma) for 1 hour at room temperature. After incubation with a specific primary antibody for NF-κB/p65 at 4°C overnight, the cells were treated with anti-rabbit IgG (H+L) antibody labelled with Alexa 488 (Molecular Probes, Waltham, Massachusetts, USA; 1:200 dilution) for 1 hour at room temperature in the dark. Then, the cells were washed

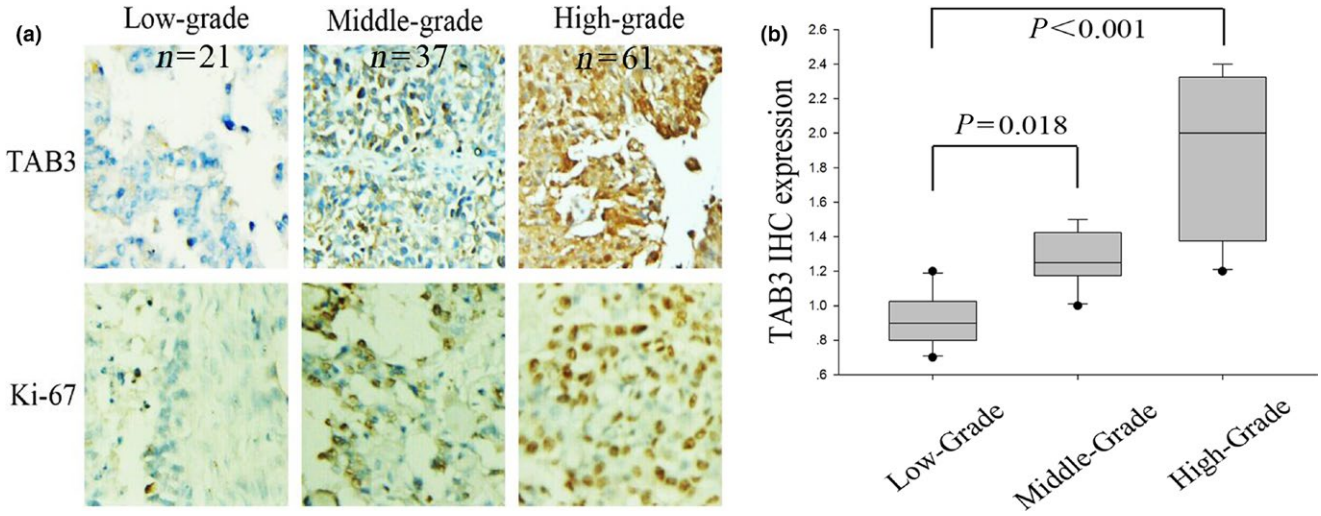

FIGURE 2 TAB3 expression and distribution was examined in EOC tissues by IHC. (a) Representative IHC images (×200) of TAB and Ki-67 protein expression in EOC tissues (from low grade to high grade) (IHC: immunohistochemical stain). (b) Box-plot presentation of TAB3 staining levels in EOC tissues with three grades. The same experiment was repeated at least three times

three times in PBS after each treatment described above. A confocal microscope (Olympus, Tokyo, Japan) was used to observe the cells.

2.12 | Statistical analysis

All the statistical analyses were performed using the SPSS 10.0 software package (SPSS, Inc., Chicago, IL, USA). The statistical significance of the correlations between TAB3 expression and clinicopathological features were analysed using Pearson χ^2 test. For the analyses of the survival data, Kaplan–Meier curves were constructed, and log-rank tests were performed. The values were expressed as the mean ± SD, and the level of significance was set at $P<.05$. Each experiment consisted of at least three replicates per condition.

3 | RESULTS

3.1 | TAB3 expression was up-regulated in EOC tissues and cell lines

To examine whether TAB3 was associated with EOC, ovarian cancer cell lines (including A2780, HO8910, OVCAR3 and SKOV3) and one normal ovarian cell line (IOSE80) were employed (Fig. 1a1, a2). Western blotting analysis showed that the protein expression of TAB3 was highly expressed in EOC cell lines. Using the same method, expression of TAB3 in 12 EOC tissues (containing three normal ovarian tissues and nine fresh ovarian tumour tissues) was detected. As shown in Fig. 1b1, b2, the expression of TAB3 protein was higher in EOC tissues compared with normal ovarian tissues. Next, quantitative real-time PCR (qRT-PCR) was assumed to detect TAB3 mRNA levels in both EOC cell lines and tissues. Clearly, comparing to normal ovarian tissues, EOC tissues showed evidently TAB3 mRNA expression. Its mRNA expression level in HO8910 and SKOV3 was significantly higher consistent with the WB results (Fig. 1c1, c2). So, in the subsequent experiments, we would adopt these two EOC cell lines. In order to confirm the association of TAB3 with EOC progression, we also examined the intracellular expression of TAB3 and Ki-67 (a cell proliferation index) in 119 specimens of EOC by immunohistochemical analysis (IHC). As expected, TAB3 expressed higher in poorly differentiated specimens compared with well-differentiated ones, which was consistent with Ki-67. The result was shown in Fig. 2.

3.2 | TAB3 expression was closely related with clinicopathological features in EOC

To further understand the clinicopathologic significance of TAB3 expression in EOC, the correlation of TAB3 expression with clinicopathologic variables was evaluated by Pearson χ^2 test. The clinicopathological data of patients are summarized in Table 1. The results of statistical analysis showed that TAB3 expression was significantly associated with histological grade, FIGO stages, lymph node metastasis and Ki-67 expression level. In addition, Spearman's correlation test showed that there was a positive correlation between the expression of TAB3 and Ki-67 ($r=.820$, $P<.001$, Fig. 3).

3.3 | TAB3 expression caused obviously adverse effects on the prognosis of EOC patients

We next evaluated whether tumour expression of TAB3 protein was associated with disease-specific survival and time to recurrence in patients. Kaplan–Meier curves for disease-specific survival revealed that TAB3 overexpression was associated with increased ovarian cancer mortality ($P<.001$) (Fig. 4a). In addition, Kaplan–Meier curves for progression-free survival revealed that TAB3 overexpression was associated with decreased relapse-free survival ($P=.004$) (Fig. 4b). To determine whether TAB3 overexpression was independently associated with patient survival, a multivariable analysis was performed. As

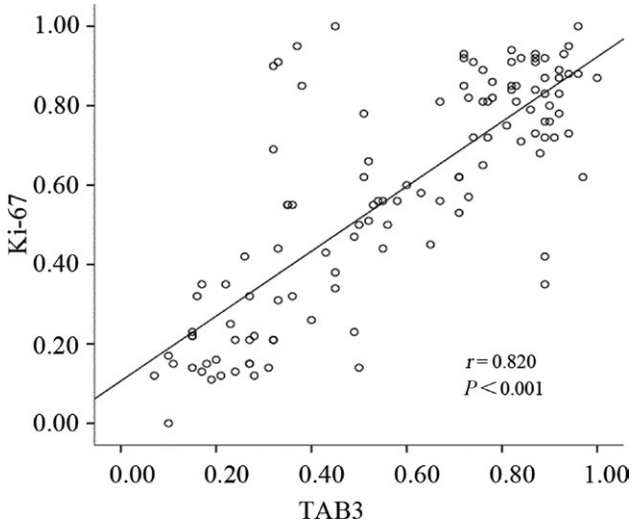

FIGURE 3 Relationship between TAB3 expression and Ki-67 proliferation index in EOC. Scatter plot of TAB3 against Ki-67 with regression line showing a correlation of them using the Spearman's correlation coefficient (r=.820, *P*<.001)

shown in Table 2, 62 of 119(52.1%) revealed high expression of TAB3, and among them, only 17 of 62(27.4%) patients of strong expression were alive. Univariate survival analysis also indicated that FIGO stage (*P*=.001), histological grade (*P*=.018), lymph node metastasis (*P*=.022), TAB3 (*P*<.001) and Ki-67 (*P*=.001) prejudiced the prognosis of patients (Table 2). Moreover, to further confirm the point, multivariate analysis using Cox's proportional hazards model showed that TAB3 (*P*=.047) as well as histological grade (*P*=.018), FIGO grade (*P*=.037) and Ki-67 expression (*P*=.027) were the four independent prognostic factors of overall survival in EOC patients (Table 3).

3.4 | Knockdown of TAB3 suppressed cell proliferation and regulated cell cycle in HO8910 and SKOV3

For the following experiments, the two EOC cell lines (HO8910 and SKOV3) were transfected with Con-shRNA, TAB3-shRNA#1, TAB3-shRNA#2 and TAB3-shRNA#3 for better digesting of the role of TAB3 in EOC cell progress, and the expression of TAB3 was assessed by WB (Fig. 5a1, a2 and b1, b2). According to the criteria described, TAB3 expression levels were substantially decreased in both HO8910 and SKOV3 cells transfected with TAB3-shRNA#1, TAB3-shRNA#2 and TAB3-shRNA#3 compared with the Con-shRNA, particularly in TAB3-shRNA#3 transfected cells. Then, in the next manipulate, the TAB3-shRNA#3 transfected cell lines was chosen to be the experimental group. Following knockdown of TAB3 gene expression with shRNA, we used the MTT assay after particular point transfection to measure changes in cell viability (Fig. 5c,d). HO8910 and SKOV3 cells treated with TAB3-shRNA#3 exhibited a declining cell viability rate compared with the negative one. To investigate the mechanism by which the proliferation of EOC cells was suppressed by the down-regulation of TAB3 expression, flow cytometry was conducted to detect the specific phase of the cell cycle. As shown in Fig. 5e1, e2 and f1, f2, knockdown of TAB3 induced EOC cell arrest in the G0/G1 phase, while in the S phase was decreased. To further confirm the above conjecture, we examined whether the expression of TAB3 was cell-cycle dependent by Western blot. As shown in Fig. 5g1, g2 and h1, h2, TAB3 expression was increased after serum addition. The expression of PCNA and CyclinD1 also had a similar trend with TAB3. In addition, knockdown of TAB3 undermined protein expression of CyclinD1 and PCNA (Fig. 5i1, i2). These results affirmed that TAB3 may be involved in the proliferation of EOC in a cell-cycle-dependent pathway.

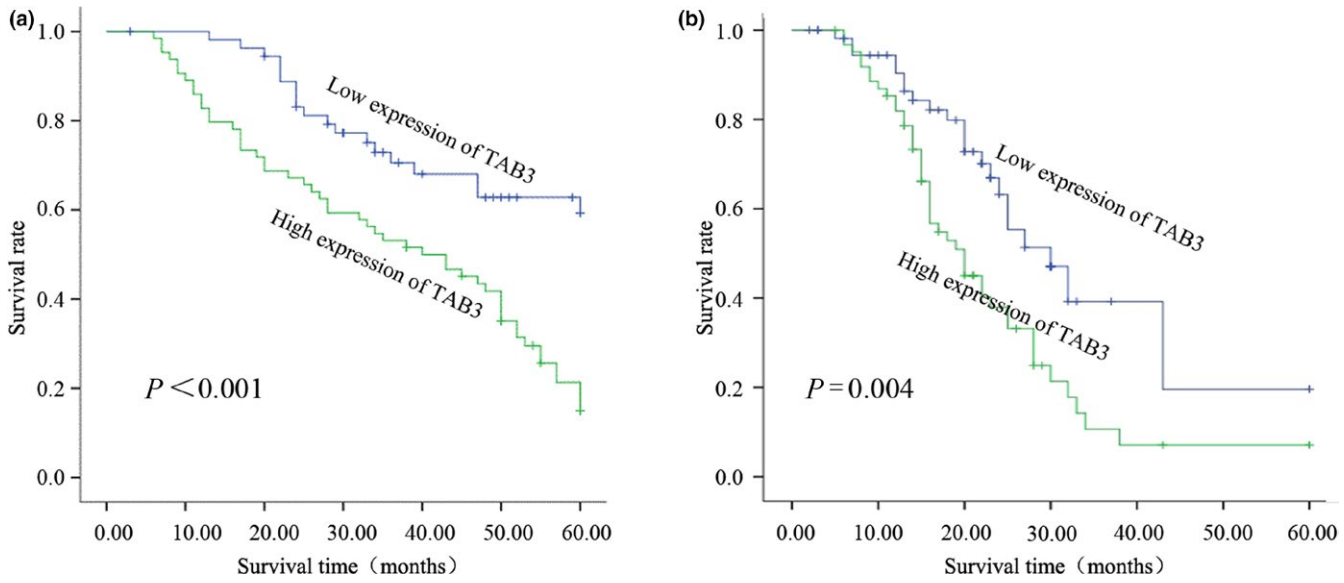

FIGURE 4 Kaplan–Meier survival curves for low versus high TAB3 expression in 119 EOC patients. (a) Kaplan–Meier curves of overall survival of patients whose ovarian tumours expressed high vs low levels of TAB3. (b) Kaplan–Meier curves of progression-free survival for patients whose ovarian tumours expressed high vs low levels of TAB3

TABLE 2 Survival status and clinicopathological characteristics in 119 EOC specimens

Characteristics	Total	Survival status		*P* value[a]
		Died	Alive	
Age (24–80 years, mean 55 years)				
≤50	40	23	17	0.750
>50	79	43	36	
FIGO stage				
I/II	59	24	35	0.001*
III/IV	60	42	18	
Histological grade				
Low	53	23	30	0.018*
High	66	43	23	
Histologic subtype				
Serous	64	33	31	0.741
Mucinous	26	16	10	
Endometrioid	15	8	7	
Clear cell	14	9	5	
Lymph node metastasis				
Negative	74	35	39	0.022*
Positive	45	31	14	
Ki-67 expression				
Low	52	20	32	0.001*
High	67	46	21	
TAB3 expression				
Low	57	21	36	0.000*
High	62	45	17	

[a]Statistical analyses were performed by the Pearson χ^2 test.
*P<.05 was considered significant.

TABLE 3 Contribution of various potential prognostic factors to survival by Cox regression analysis on 119 EOC specimens

	Hazard ratio	95% confidence interval	*P* value[a]
Histological stage	1.993	1.128–3.522	0.018*
FIGO grade	1.740	1.034–2.927	0.037*
Lymph node metastasis	1.390	0.807–2.393	0.235
TAB3 expression	0.571	0.328–0.994	0.047*
Ki-67 expression	1.862	1.073–3.231	0.027*

[a]Statistical analyses were performed by the Cox regression analysis.
*P<.05 was considered significant.

3.5 | Knockdown of TAB3 restrained resistance to chemotherapy in EOC cells

To determine whether TAB3 expression is involved in regulation of chemo-resistance in ovarian cancer, the viability of HO8910 or SKOV3 ovarian cancer cells was evaluated with TAB3 knockdown in the presence of chemotherapy reagents (cisplatin and paclitaxel). As shown in Fig. 6a1, a2 and b1, b2, the viability of HO8910 or SKOV3 cells showed a gradual decrease in a concentration-dependent manner after cisplatin and paclitaxel treatment. Knockdown of TAB3 expression in both HO8910 and SKOV3 cells further decreased the viability, indicating a significant increase in the drug sensitivity. To further confirm whether the growth inhibition in EOC cells was related to apoptosis, we evaluated the apoptosis effect of TAB3-shRNA#3 on cell lines. As shown in Fig. 6c1, c2 and d1, d2, after treatment of the cells with TAB3-shRNA#3, the percentage of apoptotic cells increased in both cell lines. It was common knowledge that mitochondrial apoptosis pathway leaded to caspase activation and induced cell death. We next determined whether this situation was also involved in TAB3-induced EOC cells. Cells were treated with homologous plasmids, and cleaved caspase 3, 9 and Bcl-2 proteins were determined by WB. From Fig. 6e1, e2 and f1, f2, we observed a comparative increase in the expression of cleaved caspase proteins in both cell lines in response to TAB3-shRNA#3. TAB3-shRNA#3 reduced Bcl-2 protein expression (Fig. 6e1, e2 and f1, f2). It might explain such a problem that cell-cycle arrest and mitochondrial apoptosis may be major mechanisms to inhibit cell proliferation in TAB3-shRNA-treated EOC cells. These results suggested that TAB3 expression positively correlated with expression of drug transporters and resistance to chemotherapeutic reagents in EOC cells.

3.6 | TAB3 regulated EOC cell bioactivity and chemotherapy performance *via* the NF-κB pathway

We next investigated whether TAB3 affected EOC cell bioactivity and chemotherapy performance *via* the NF-κB signalling. As shown in Fig. 7a1, a2, silencing TAB3 expression resulted in prolonged IκBα activation and accelerated degradation of IκBα. Consistently, when transfected with the TAB3-shRNA#3 plasmid, p65 and its phosphorylation expression was significantly down-regulated. After transfected for 36 hours, the nuclei of HO8910 cells were stained blue and the NF-κB/p65 proteins were stained red. As shown in Fig. 7b, knockdown of TAB3 expression by shRNA-mediated RNAi inhibited the translocation of NF-κB/p65 from the cytoplasm to the nucleus. All these results suggested that TAB3 regulated EOC cell bioactivity and chemotherapy performance *via* the NF-κB pathway. To further conform the above conclusion, the viability of HO8910 cell line was evaluated with TAB3 knockdown or p65 overexpression in the presence of chemotherapy reagents paclitaxel or cisplatin.

As shown in Fig. 7c1, c2, the viability analysis showed a gradual decrease with increasing concentrations of paclitaxel or cisplatin. Knockdown of TAB3 expression further decreased the tendency. On the contrary, overexpression of p65 increased the resistance to paclitaxel or cisplatin treatment. Apart from this, TAB3-shRNA#3 promoted cell apoptosis, while p65 overexpression would greatly reduce this effectiveness (Fig. 7d1 and d2).

TAB3 has recently been described as a functional homologue of TAB2. The formation of a TRAF6-TAB3-TAK1 complex may cause conformational changes in the catalytic domain of TAK1, thereby inducing the activation of the NF-κB pathway. To ascertain whether TRAF6

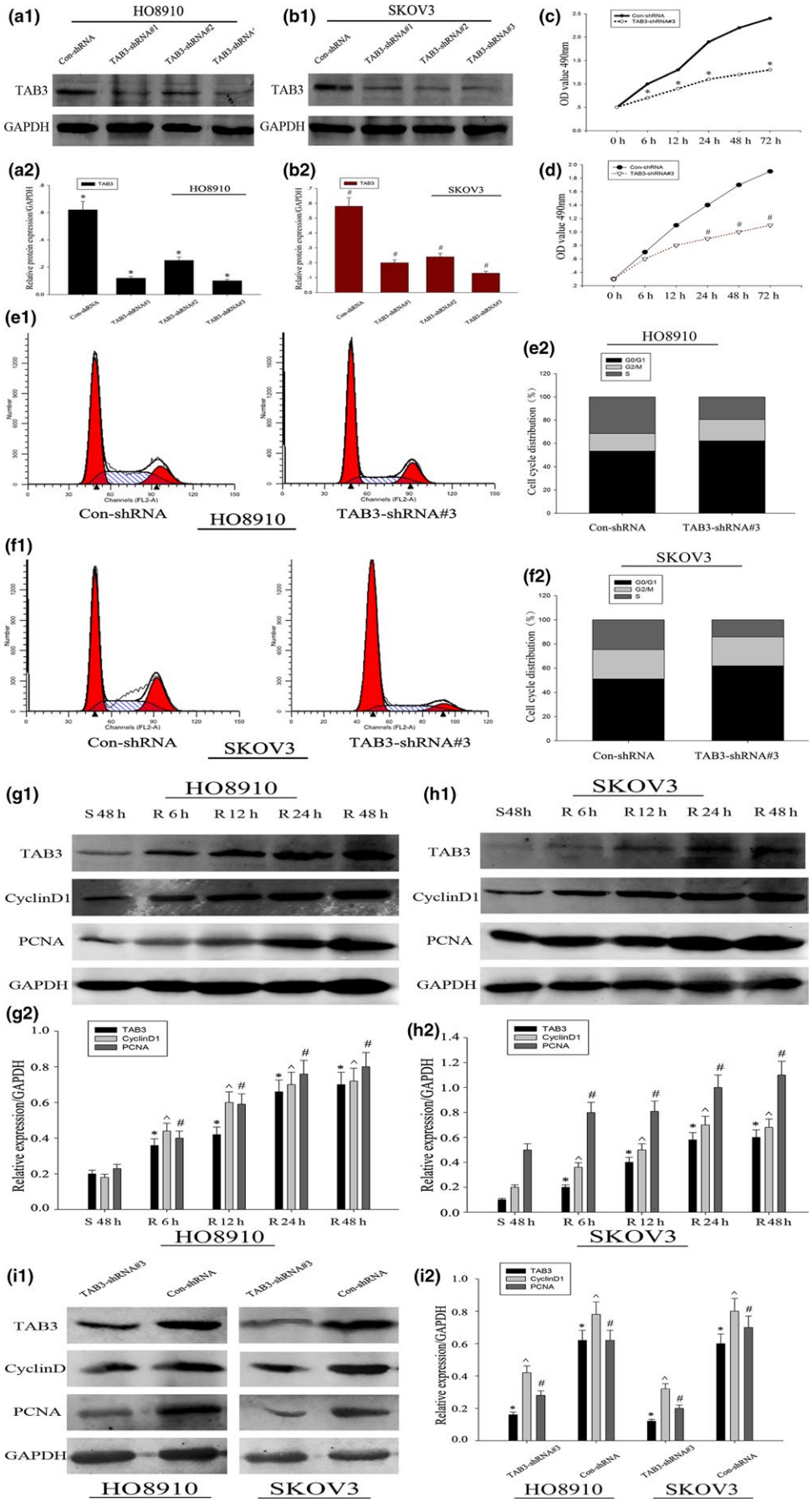
(a1)
HO8910
Con-shRNA
TAB3-shRNA#1
TAB3-shRNA#2
TAB3-shRNA#3
TAB3
GAPDH
(b1)
SKOV3
(c)
OD value 490nm
0 h 6 h 12 h 24 h 48 h 72 h
(a2)
Relative protein expression/GAPDH
(b2)
(d)
(e1)
Number
Channels (FL2-A)
Con-shRNA
HO8910
TAB3-shRNA#3
(e2)
G0/G1
G2/M
S
Cell cycle distribution (%)
(f1)
SKOV3
(f2)
(g1)
S 48 h R 6 h R 12 h R 24 h R 48 h
CyclinD1
PCNA
(h1)
(g2)
Relative expression/GAPDH
(h2)
(i1)
CyclinD
(i2)

FIGURE 5 ShRNA-directed knockdown of TAB3 expression inhibited cell proliferation and blocked cell cycle in HO8910 and SKOV3 cell lines. (a1, a2 and b1, b2) TAB3 expression of EOC cell lines was detected in groups after different transfections, which resulted in the differential expression of TAB3 among the groups in each different EOC cell lines. (c and d) The viability of EOC cell lines was evaluated by MTT assay. The data need to be labelled as the mean ± SEM. (e1, e2 and f1, f2) Cell-cycle profile was examined by flow cytometry and percentages of cells in G0/G1, S and G2/M phase in the TAB3-shRNA#3 were compared with the Con-shRNA group. (g1, g2 and h1, h2) HO8910 and SKOV3 cells were harvested and analysed for TAB3, and cell-cycle-related molecules including PCNA and CyclinD1 expression following the serum starvation and refeeding experiment. Mean ± SEM of three independent experiments (n=3, $P<.05$). (i1, i2) Protein expressions of TAB3, PCNA and CyclinD1 were examined by WB in TAB3-shRNA#3 and Con-shRNA cell lines

and TAK1 are required for TAB3 induced NF-κB activation, we used siRNA to silence the expression of TRAF6 or TAK1 in cells. As shown in Fig. 7e1 and e2, knockdown of TRAF6 or TAK1 expression significantly inhibited p65 and p-p65 activation, and knockdown of TRAF6, TAK1 and TAB3 had the strongest suppression utility, suggesting that TAB3 activates NF-κB through the canonical TRAF6-TAK1-dependent pathway.

4 | DISCUSSION

It has been well demonstrated that the transcription factor NF-κB plays a pivotal role in the regulation of diverse physiological and pathological processes, including immune response, inflammation and cancer development.[18] In order to keep homeostasis, NF-κB activation

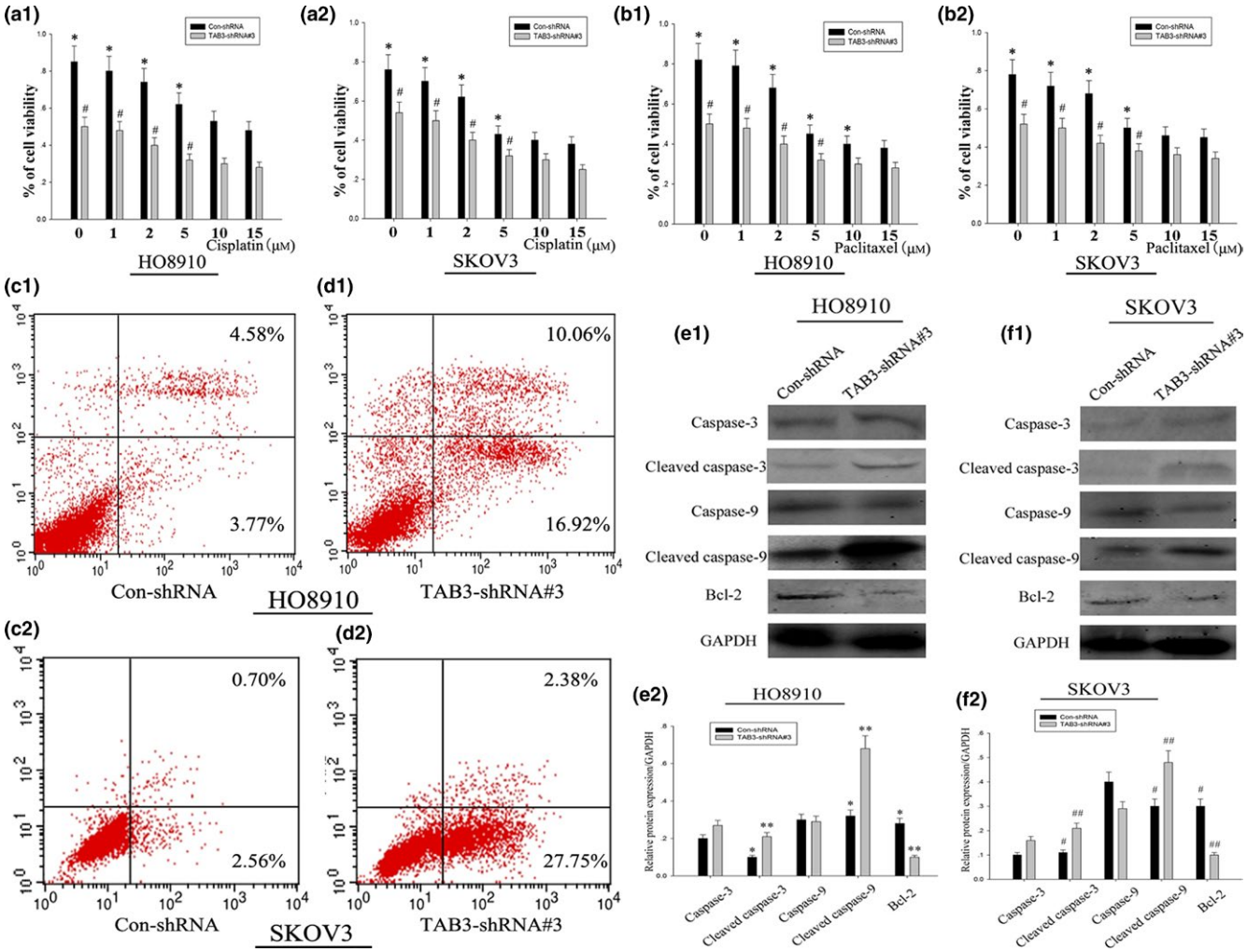

FIGURE 6 Knockdown of TAB3 expression restrained the resistance of EOC cells to chemotherapeutic drugs. (a1, a2 and b1, b2) The viability of HO8910 and SKOV3 cell lines with or without TAB3 knockdown (TAB3-shRNA#3) was measured by MTT assay after treatment with indicated concentrations of cisplatin and paclitaxel. Data are presented as mean ± SD. (c1, c2 and d1, d2) HO8910 and SKOV3 cell lines were treated with Con-shRNA and TAB3-shRNA#3, respectively. Apoptosis was examined by Annexin V assay in Cellometer. (e1, e2 and f1, f2) Caspase-3, Caspase-9 and Bcl-2 were determined by WB after transfecting corresponding plasmids for 24 h. As protein expression of TAB3 decreased, these apoptosis indexes changed significantly

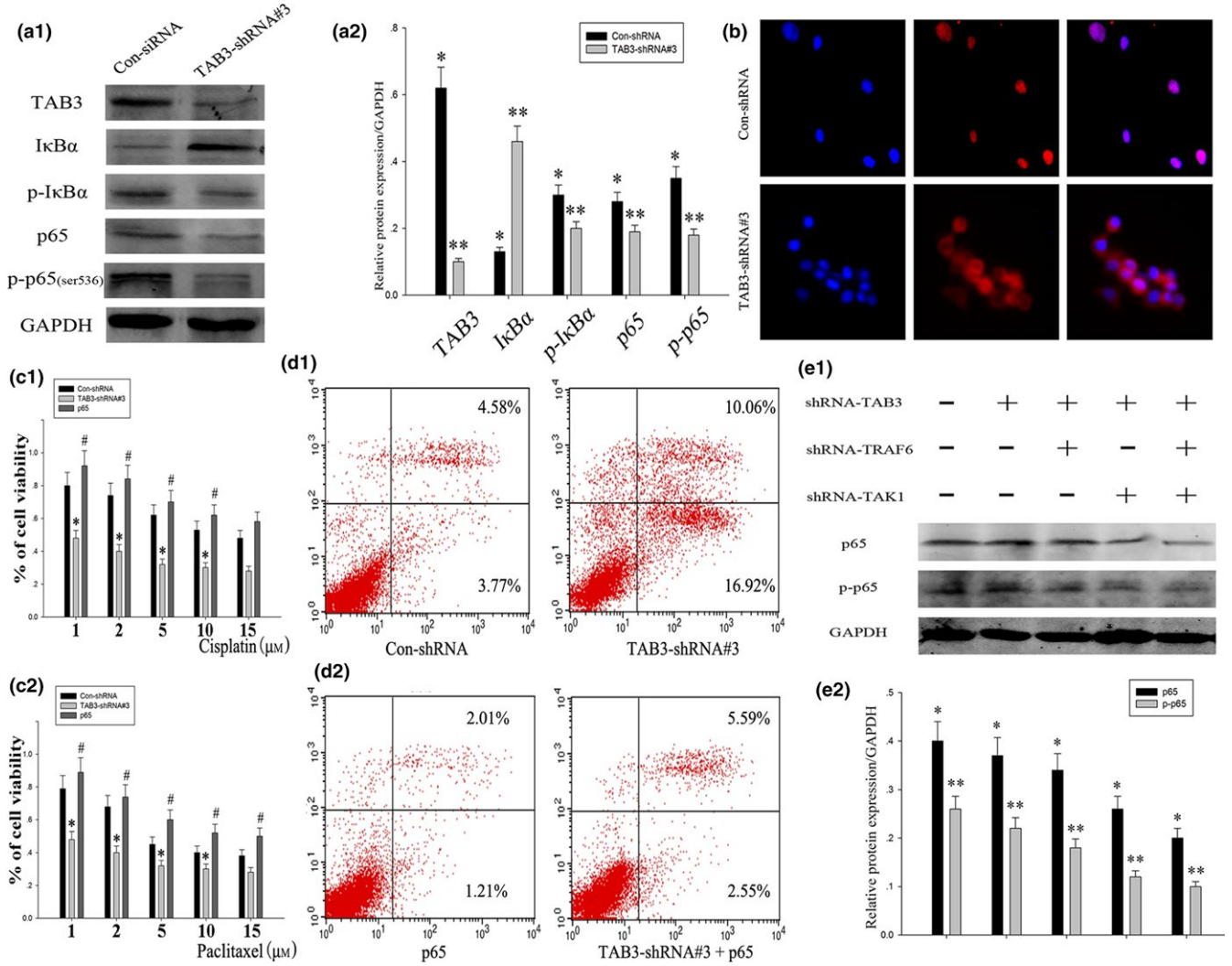

FIGURE 7 TAB3 regulated EOC cell bioactivity and chemotherapy performance *via* the NF-κB pathway. (a1 and a2) HO8910 cells were transfected with Con-shRNA and TAB3-shRNA#3. After 36 h, the cells were collected, and the whole cell lysates were analysed by WB with the indicated antibodies. (b) The blue areas indicated nuclei stained using 4, 6-diamidino-2-phenylindole (DAPI), and the red areas indicated the nuclear translocation of NF-κB/p65 in HO8910 cells transfected with different plasmids. (c1 and c2) The viability of HO8910 ovarian cancer cells with TAB3 knockdown or p65 overexpression was measured by MTT assay after treatment of cells with indicated concentrations of paclitaxel or cisplatin. Data are presented as mean ± SD. $P<.05$. (d1 and d2) HO8910 cell line was treated with Con-shRNA, TAB3-shRNA#3, p65 overexpression and the mixed plasmid. Apoptosis was examined by Annexin V assay in Cellometer. (e1 and e2) HO8910 cell lines were transfected with shRNA-TAB3, shRNA-TRAF6 and shRNA-TAK1, the measurement of immunoblotting were carried out 48 h post transfection

process must be tightly controlled. Irrational activation of NF-κB not only takes part in tumorigenesis but also is relevant to adverse clinicopathological features in patients, such as lymphatic metastasis, resistance to chemotherapeutic treatments and poor prognosis.[19]

In the previous reports, the materiality for NF-κB in the development of ovarian cancer was vetter widely known worldwide. Ovarian cancer has the highest mortality rate of all gynaecologic cancers, and up to 75% of patients are diagnosed at an advanced stage. It is difficult to make a straightforward diagnosis without definite symptoms and effective screening methods.[5] Meanwhile, the molecular mechanisms underlying ovarian cancer are poorly understood. Resistance to chemotherapeutic drugs is the primary reason why ovarian cancer is such a deadly malignancy.[20] The molecular pathways that can lead to resistance are varied. Cisplatin may be the most universal chemotherapeutic drug in the treatment of OC in clinic. Study has also showed that cisplatin could induce NF-κB activation in EOC cells. A combination of cisplatin and NF-κB decoy, a NF-κB inhibitor, enhanced tumour cell death.[21]

Further, NF-κB and IKK complex activation relies on an upstream kinase complex, which consisted of TAK1 and adaptor proteins TAB1, TAB2 and TAB3.[22,23] Since TAB3 is an adaptor protein important for maintenance of homeostasis through regulating expression of proinflammatory cytokines.[24] Recent emerging evidence indicates that TAB3 also plays a crucial role in cancer development, taking HCC, for example, which enhances the importance of TAB3 as a promising clinical therapeutic candidate.[25] Meanwhile, TAB3 is highly expressed in

NSCLC tissues and speculated to be a therapy target for NSCLC.[16] However, whether TAB3 is related to the progress of EOC and its molecular mechanism still remains unclear.

In this study, we demonstrated that TAB3 was up-regulated in EOC cells and tissues. The up-regulation of TAB3 expression in EOC correlates with histological grade, FIGO stages, lymph node metastasis and predicted poor prognosis of patients. Also, by Kaplan–Meier survival analysis, TAB3 was demonstrated to predict poor survival in EOC patients. In addition, multivariate analysis suggested that TAB3 expression was related to high-risk clinical parameter, and it was identified as an independent prognostic factor for overall survival in EOC. To further investigate whether TAB3 could be used as a potential therapeutic target, we constructed specific TAB3 shRNA plasmids and transfected them into EOC cells. We found that knockdown of TAB3 suppressed the proliferation. In addition, ectopic TAB3 promoted antiapoptotic factor expression and inhibited pro-apoptotic factor expression. Our further analysis found TAB3 could activate NF-κB pathway whose target genes are critical for apoptosis.

It is a consensus that chemoresistance remains to be a major clinical challenge and great obstacle for current OC therapy. Chemotherapy induces tumour cells to demise largely by activating apoptosis-related routines, since inhibition of apoptosis will increase tumour cells resistant to anti-tumour treatment. Multiple genes, which are related to apoptosis resistance, have been found to lead to chemoresistance.[26] In our study, we determined that knockdown of TAB3 weakens cisplatin and paclitaxel resistance, indicating its function and potential utilization in EOC chemotherapeutic treatment. It has also been found that some molecular dysregulation causes apoptotic dysregulation, including activation of antiapoptotic factor, such as Bcl-2; inactivation of pro-apoptotic effectors, such as p53 and Caspases; or induction of survival signals, including survivin and NF-κB.[27] The genes modulating chemoresistance also regulate the apoptotic-related factors. For examples, Bmi-1 is reported to promote apoptotic resistance *via* activating NF-κB and inducing expression of NF-κB-targeted genes.[28] Our study confirmed that TAB3 knockdown pro-apoptotic factor expression, such as Caspase-3 and Caspase-9, and inhibited enhanced antiapoptotic factor expression, such as Bcl-2. We further analysed the mechanism and found TAB3 activated NF-κB pathway, knockdown of TAB3 could promote p65 translocate to the cytoplasm, which is a marker for inactivating NF-κB pathway. Furthermore, TAB3 activates NF-κB through the canonical TRAF6-TAK1-dependent pathway. All these results encourage us to make such a conclusion that loss of TAB3 expression by shRNA exhibits suppressive bioactivity and increased chemical sensitivity of ovarian cancer cell lines *via* the NF-κB pathway.

In summary, our study demonstrates that TAB3, which is highly expressed in EOC cells and tissues, promotes the resistance to cisplatin, mechanism analysis found it activated NF-κB pathway to inhibit apoptosis. Our study reveals that the TAB3 is an important carcinogen in EOC development, and the findings have therapeutic potential for developing treatment of tumour patients.

CONFLICT OF INTEREST

The authors declare no conflicts of interest.

REFERENCES

1. English DP, Menderes G, Black J, Schwab CL, Santin AD. Molecular diagnosis and molecular profiling to detect treatment-resistant ovarian cancer. *Expert Rev Mol Diagn*. 2016;16:769–782.
2. Siegel RL, Miller KD, Jemal A. Cancer statistics, 2015. *CA Cancer J Clin*. 2015;65:5–29.
3. Winterhoff B, et al. Molecular classification of high grade endometrioid and clear cell ovarian cancer using TCGA gene expression signatures. *Gynecol Oncol*. 2016;141:95–100.
4. Mirandola L, et al. Cancer testis antigens: novel biomarkers and targetable proteins for ovarian cancer. *Int Rev Immunol*. 2011;30:127–137.
5. Krzystyniak J, et al. Epithelial ovarian cancer: the molecular genetics of epithelial ovarian cancer. *Ann Oncol*. 2016;27(Suppl 1):i4–i10.
6. Hu Y, et al. The importance of toll-like receptors in NF-kappaB signaling pathway activation by *Helicobacter pylori* infection and the regulators of this response. *Helicobacter* 2016; doi: 10.1111/hel.12292.
7. Muller CW, Harrison SC. The structure of the NF-kappa B p50:DNA-complex: a starting point for analyzing the Rel family. *FEBS Lett*. 1995;369:113–117.
8. Chiu CF, et al. NF-kappaB-driven suppression of FOXO3a contributes to EGFR mutation-independent gefitinib resistance. *Proc Natl Acad Sci U S A*. 2016;113:E2526–E2535.
9. Mishra V, et al. Titanium dioxide nanoparticles augment allergic airway inflammation and Socs3 expression via NF-kappaB pathway in murine model of asthma. *Biomaterials*. 2016;92:90–102.
10. Weaver KD, et al. Potentiation of chemotherapeutic agents following antagonism of nuclear factor kappa B in human gliomas. *J Neurooncol*. 2003;61:187–196.
11. Zhang W, et al. Interleukin-1 receptor-associated kinase-2 genetic variant rs708035 increases NF-kappaB activity through promoting TRAF6 ubiquitination. *J Biol Chem*. 2014;289:12507–12519.
12. Wei H, et al. PRMT5 dimethylates R30 of the p65 subunit to activate NF-kappaB. *Proc Natl Acad Sci U S A*. 2013;110:13516–13521.
13. Heo KS, et al. Phosphorylation of protein inhibitor of activated STAT1 (PIAS1) by MAPK-activated protein kinase-2 inhibits endothelial inflammation via increasing both PIAS1 transrepression and SUMO E3 ligase activity. *Arterioscler Thromb Vasc Biol*. 2013;33:321–329.
14. Ye JS, et al. Lysine 63-linked TANK-binding kinase 1 ubiquitination by mindbomb E3 ubiquitin protein ligase 2 is mediated by the mitochondrial antiviral signaling protein. *J Virol*. 2014;88:12765–12776.
15. Zhao N, et al. MicroRNA-26b suppresses the NF-kappaB signaling and enhances the chemosensitivity of hepatocellular carcinoma cells by targeting TAK1 and TAB3. *Mol Cancer*. 2014;13:35.
16. Chen J, et al. TAB3 overexpression promotes cell proliferation in non-small cell lung cancer and mediates chemoresistance to CDDP in A549 cells via the NF-kappaB pathway. *Tumour Biol*. 2016;37:3851–3861.
17. Tao T, et al. TAB3 O-GlcNAcylation promotes metastasis of triple negative breast cancer. *Oncotarget*. 2016;7:22807–22818.
18. Stouch AN, et al. IL-1beta and inflammasome activity link inflammation to abnormal fetal airway development. *J Immunol*. 2016;196:3411–3420.
19. Arase N, et al. The effect of rhododendrol inhibition of NF-kappaB on melanocytes in the presence of tyrosinase. *J Dermatol Sci*. 2016;83:157–159.
20. Lorenzato A, et al. The integrin-linked kinase-associated phosphatase (ILKAP) is a regulatory hub of ovarian cancer cell susceptibility to platinum drugs. *Eur J Cancer*. 2016;60:59–68.
21. Kasparkova J, et al. Different affinity of nuclear factor-kappa B proteins to DNA modified by antitumor cisplatin and its clinically ineffective trans isomer. *FEBS J*. 2014;281:1393–1408.

22. Gill JS, Windebank AJ. Ceramide initiates NFkappaB-mediated caspase activation in neuronal apoptosis. *Neurobiol Dis*. 2000;7:448–461.
23. Emmerich CH, et al. Activation of the canonical IKK complex by K63/M1-linked hybrid ubiquitin chains. *Proc Natl Acad Sci U S A*. 2013;110:15247–15252.
24. Hu MM, et al. TRIM38 inhibits TNFalpha- and IL-1beta-triggered NF-kappaB activation by mediating lysosome-dependent degradation of TAB2/3. *Proc Natl Acad Sci U S A*. 2014;111:1509–1514.
25. Roh YS, Song J, Seki E. TAK1 regulates hepatic cell survival and carcinogenesis. *J Gastroenterol*. 2014;49:185–194.
26. Yang X, et al. Pinin associates with prognosis of hepatocellular carcinoma through promoting cell proliferation and suppressing glucose deprivation-induced apoptosis. *Oncotarget*. 2016; doi: 10.18632/oncotarget.9233.
27. Jaiswal D, et al. Dysregulation of apoptotic pathway candidate genes and proteins in infertile azoospermia patients. *Fertil Steril*. 2015;104:736–743 e6.
28. Zhu DD, et al. Significance of NF-kappaB activation in immortalization of nasopharyngeal epithelial cells. *Int J Cancer*. 2016;138:1175–1185.